

1 **Increased inorganic aerosol fraction contributes to air pollution and**  
2 **haze in China**

Yonghong Wang<sup>1,2</sup>, Yuesi Wang<sup>1,6</sup>, Lili Wang<sup>1</sup>, Tuukka Petäjä<sup>2,3</sup>, Qiaozhi  
Zha<sup>2</sup>, Chongshui Gong<sup>1,4</sup>, Sixuan Li<sup>7</sup>, Yuepeng Pan<sup>1</sup>, Bo Hu<sup>1</sup>, Jinyuan Xin<sup>1</sup> and  
Markku Kulmala<sup>2,3,5</sup>

3 <sup>1</sup>State Key Laboratory of Atmospheric Boundary Layer Physics and Atmospheric Chemistry  
4 (LAPC), Institute of Atmospheric Physics, Chinese Academy of Sciences, Beijing 100029,  
5 China

6 <sup>2</sup>Institute for Atmospheric and Earth System Research / Physics, Faculty of Science, P.O.Box  
7 64, 00014 University of Helsinki, Helsinki, Finland

8 <sup>3</sup>Joint international research Laboratory of Atmospheric and Earth SysTem sciences  
9 (JirLATEST), Nanjing University, Nanjing, China

10 <sup>4</sup>Institute of Arid meteorology, China Meteorological Administration, Lanzhou 730000,  
11 China

12 <sup>5</sup>Aerosol and Haze Laboratory, Beijing Advanced Innovation Center for Soft Matter Science  
13 and Engineering, Beijing University of Chemical Technology (BUCT), Beijing, China

14 <sup>6</sup>Centre for Excellence in Atmospheric Urban Environment, Institute of Urban Environment,  
15 Chinese Academy of Science, Xiamen, Fujian 361021, China

16 <sup>7</sup>State Key Laboratory of Numerical Modeling for Atmospheric Sciences and Geophysical  
17 Fluid Dynamics (LASG), Institute of Atmospheric Physics, Chinese Academy of Sciences,  
18 Beijing 100029, China

19 Revised to: Atmospheric Chemistry and Physics

20 Corresponding authors: Y.S. Wang, L.L.Wang and M. Kulmala

21 E-mail: [wys@mail.iap.ac.cn](mailto:wys@mail.iap.ac.cn); [wll@mail.iap.ac.cn](mailto:wll@mail.iap.ac.cn); [markku.kulmala@helsinki.fi](mailto:markku.kulmala@helsinki.fi)

## 22 **Abstract**

23 The detailed formation mechanism of increased number of haze events in China is  
24 still not very clear. Here, we found that reduced surface visibility and an increase in  
25 satellite derived columnar concentration of inorganic precursor concentrations are  
26 connected with each other. Typically higher inorganic mass fractions lead to increased  
27 aerosol water uptake and light scattering ability in elevated relative humidity. Satellite  
28 observation of aerosol precursors of NO<sub>2</sub> and SO<sub>2</sub> showed increased concentrations  
29 during study period. Our in-situ measurement of aerosol chemical composition in  
30 Beijing also confirmed increased contribution of inorganic aerosol fraction as a function  
31 of increased particle pollution level. Our investigations demonstrate that the increased  
32 inorganic fraction in the aerosol particles is a key component in the frequently occurring  
33 haze days during studying period, and particularly the reduction of nitrate, sulfate and  
34 their precursor gases would contribute towards better air quality in China.

## 35 **Introduction**

36 As one of the most heavily polluted regions in the world, China has suffered from  
37 air pollution for decades (Hao et al., 2007; Zhang et al., 2015). Aerosol particles, as  
38 major air pollutant, have significant effects on human health (Lelieveld et al., 2015).  
39 The general public and the central government in China have realized the severe  
40 situation and have taken some measures to improve the air quality nationwide in the  
41 recent years. For example, the state council published a plan for air pollution control,  
42 in September of 2013, aim to reduce PM<sub>2.5</sub> concentrations by 10%~25% in different  
43 regions of China. The successful implementation requires a sufficient knowledge of

44 haze formation mechanism (Kulmala, 2015) and comprehensive observation network  
45 (Kulmala, 2018). Our understanding on haze events with high PM<sub>2.5</sub> concentrations in  
46 China is still limited due to the spatial-temporal variation of aerosol properties and  
47 limited observation information (Wang et al., 2016). Recent studies found that  
48 secondary aerosol components are important during the intense haze events in Beijing,  
49 Xi'an, Chengdu and Guangzhou during January of 2013, and the reduction of aerosol  
50 precursors is a key step to reduce particle pollution (Guo et al., 2014; Huang et al.,  
51 2014). The analysis of longer time series data from Nanjing shows that secondary  
52 particles are typically dominating even the number concentrations in polluted  
53 conditions (Kulmala M., 2016). The most abundant mass fractions of atmospheric  
54 aerosol are inorganic and organic components, which have large spatio-temporal  
55 variation (Jimenez et al., 2009). Identifying the most abundant as well as critical aerosol  
56 species that contribute to the haze formation in a longtime perspective is important to  
57 draw up effective plans for the air pollution control.

58 Here, a comprehensive data sets were used to reveal that an increasing trend of  
59 inorganic components in atmospheric aerosol may be a pivotal factor, at least, which  
60 leads to frequently occurred haze events in China from 1980-2010. We suggests that  
61 the controlling of inorganic aerosol components of nitrate, sulfate and their precursors  
62 should be of a high priority due to their strong water uptake abilities and therefore, light  
63 scattering ability in high RH conditions.

## 64 **2.Methodology**

65 The daily averaged visibility and relative humidity data in 262 sites of China are  
66 obtained from the Integrated Surface Dataset (ISD) from National Oceanic and  
67 Atmospheric Administration National Climate Data Center of the USA

68 (<https://www.ncdc.noaa.gov/isd>). The visibility observations were made three times a  
69 day at 8-hour intervals begins at 00:00 by well trained technicians. They measured  
70 visual range using distinctive markers, such as tall buildings, mountains and towers,  
71 to which the distance from the meteorological monitoring stations are known. First,  
72 we quantified the importance of relative humidity to visibility as the hygroscopic  
73 inorganic compounds typically grow in size in high humidity (Swietlicki et al., 2008).  
74 Aerosol size growth and composition change in high humidity condition are highly  
75 related light scattering ability (Zhang et al., 2015). Studies always use  $f(RH)$ , a  
76 parameter which is defined as the ratio of light scattering coefficient under high RH  
77 with that under low RH.  $f(RH)$  is a unitless number, usually ranges from one to two.  
78 At ambient RH around 80%, a higher  $f(RH)$  value usually corresponds to higher  
79 inorganic aerosol fraction, while a lower value usually corresponds to high organic  
80 fraction. The reason is that inorganic aerosol compounds of nitrate, sulfate and  
81 ammonium have more strong water uptake ability than organic compounds. In  
82 addition, the high humidity condition in ambient prefers the formation of inorganic  
83 aerosol from precursors of  $NO_2$  and  $SO_2$  (Wang et al., 2014). In this study, for a given  
84 site and given year, we defined a  $f(RH)$ -like parameter,  $R_i$ , using the observed annual  
85 visibility ( $V$ ) as a ratio ( $R_i$ ) between visibility values from the surface observation  
86 stations, when the daily average RH was below 40% for more than 20 days. In the  
87 corresponding high-humidity cases daily RH was between 80%~90% for more than  
88 20 days each year at a given observation site:

89

90 
$$R_i = \frac{V_{dry}}{V_{wet}}.$$

91 We use this ratio to infer long trend of aerosol hygroscopicity information. In  
92 addition, we calculate anomaly (A) from the ratio for a given year  $i$  as a difference from  
93 the 30-year ( $R_{30y}$ ) from 1980 to 2010:

$$94 \quad A = R_i - R_{30y}.$$

95 Our spatial focus is placed on North China Plain, Yangtze River Plain and Sichuan  
96 Basin due to frequent haze events (Zhang et al., 2012). The stations in Pearl River delta  
97 region and other Southern China stations were not included due to limited days with  
98 the daily average RH below 40%.

99 The atmospheric column amount of  $\text{NO}_2$  and  $\text{SO}_2$  data are obtained from  
100 SCIAMACHY (Scanning Imaging Absorption spectrometer for Atmospheric  
101 CHartography) satellite products. Modeled aerosol chemical composition from GEOS  
102 (Goddard Earth Observing System) - Chem chemical transport model in China during  
103 1998-2012 is used. The model utilizes assimilated meteorology data and regional  
104 emission inventories with a horizontal resolution of  $2^\circ \times 2^\circ$  with 47 vertical levels from  
105 surface to 80 km. The detailed information about the model can be found in (Boys et  
106 al., 2014). Aerosol chemical composition of organic, sulfate, nitrate, ammonium and  
107 chloride were measured with a high-resolution-time of flight-aerosol mass  
108 spectrometers (DeCarlo et al., 2006). Detailed information of data analysis, collection  
109 efficiencies (CE) and relative ionization efficiencies are presented in Zhang et al. (2014).

### 110 **3. Results and discussion**

#### 111 **3.1 Decreasing trend in visibility in high relative humidity conditions**

112 According to the geographical division, our study sites are mainly in North China  
113 Plain (NCP), Sichuan Basin (SCB) and Yangtze River Plain (YRP) as showed in Figure

114 1. The average visibility in low RH in NCP, SCB, YRP and China are 18.2 km, 21.4  
115 km, 19.5 km and 23.3 km, while in high RH conditions are 10.6 km, 13.7 km, 13.7 km  
116 and 17.4 km, respectively. In general, visibility in low RH condition has fluctuated  
117 trend, particularly in Northern China Plain, Sichuan Basin and Yangtze river Plain  
118 region, whereas visibility in high RH conditions showed decreasing trend as shown in  
119 Figure S1 (a) and (b). The average ratio of visibility in low RH to that in high RH from  
120 1980-2010 is presented in Figure 1. The maximum ratios were identified in eastern  
121 China and in some western Chinese cities. Three heavily polluted regions, Northern  
122 China Plain, Sichuan Basin and Yangtze river Plain were identified based on values of  
123 high  $R_i$ , which are also constant with aerosol mass concentrations and haze day  
124 distributions (van Donkelaar et al., 2010; Xin et al., 2015). That is, the higher ratios  
125 occurred in more severe air pollution areas, like North China Plain, Sichuan Basin and  
126 the city of Urumqi, where the contribution of hygroscopic aerosol is more pronounced  
127 in comparison with non-hygroscopic dust particles. The average  $R_i$  during 1980-1984  
128 in Northern China Plain, Sichuan Basin and Yangtze river Plain are 1.62, 1.41, 1.29  
129 and 1.31, respectively, contrasting with the values of 1.98, 1.81, 1.70 and 1.52 during  
130 2006-2010. The increments are 22.3%, 27.3%, 31% and 16%, respectively. It is worth  
131 noting that the  $R_i$  in Yangtze river Plain region exhibits the most increment, which  
132 implies the increased emissions with rapid economic growth. Long time trends of this  
133 ratio in a specific site can reveal the variation of aerosol inorganic fraction and organic  
134 fraction due to their different hygroscopicity and water uptake capacity and associated  
135 light extinction ability. That is, the mass fractions and concentrations of sulfate, nitrate  
136 and ammonium may have increased over study period as they dominate water uptake  
137 ability compared with other components (e.g., organic, black carbon, dust and metal  
138 elements, see Table S1) in the atmospheric aerosol (Wang et al., 2015). For the selected

139 regions, we have calculated the anomaly as a regional average as shown in Figure 2.  
140 The ratio showed increasing trends over three regions of China and the maximum  
141 trends occurred in North China Plain with the value of 0.0168 per year, which indicate  
142 an increase of hygroscopic aerosol in these regions during the 30-year observation  
143 period.

144 To corroborate our results, Yang et al. (2011) showed an increasing fraction of  
145 inorganic components by 20% in Beijing from 1998 to 2008 using in-situ offline  
146 measurement, especially in summer, while the fractions of hydrophobic components  
147 such as organic and black carbon decreased in the aerosol phase. A recent study by  
148 Boys et al. (2014) revealed that increasing fraction of secondary inorganic aerosol is  
149 dominated in the increased mass concentration of PM<sub>2.5</sub> in China from 1998-2012 using  
150 GEOS-Chem model results. By using observed meteorology data sets, Fu et al. (2014)  
151 revealed that the number of haze days have significantly increased in the past three  
152 decades over North China Plain due to the increase in hygroscopic inorganic aerosol  
153 composition.

### 154 3.2 Enhanced emissions of inorganic aerosol precursors

155 The longterm trends of aerosol precursors and their spatial variability can improve  
156 our understanding of the trends in aerosol chemical composition. Figure 3 and Figure  
157 4 show atmospheric column trends of NO<sub>2</sub> and SO<sub>2</sub> observed from SCIAMACHY. The  
158 column NO<sub>2</sub> level can be a good proxy for vehicle and coal burning emission associated  
159 with oil and coal consumption (Richter et al., 2005). The column amount of NO<sub>2</sub>  
160 showed pronounced increasing trends in three regions of China, particularly in Northern  
161 China with the value of  $0.14 \times 10^{15}$  molecule/cm<sup>2</sup>/year from 2002 to 2011. This is  
162 probably associated with the increase in power plant and on-road vehicle emissions

163 (Wu et al., 2012). The average NO<sub>2</sub> concentration in Northern China increased by more  
164 than two-fold, while in the Yangze River Plain region experienced a considerable  
165 smaller trend in NO<sub>2</sub>, with the value of  $9.7 \times 10^{15}$  molecule/cm<sup>2</sup> in 2010 and  $6.4 \times 10^{15}$   
166 molecule/cm<sup>2</sup> in 2002. As a whole, the column NO<sub>2</sub> concentration in China doubled  
167 from 2002 to 2010, with the values of  $1.4 \times 10^{15}$  molecule/cm<sup>2</sup> in 2002 and  $2.8 \times 10^{15}$   
168 molecule/cm<sup>2</sup> in 2010, respectively.

169 Figure 4 depicts trend in SO<sub>2</sub> concentration in four regions of China from 2004 to  
170 2010. The SO<sub>2</sub> concentration showed an increasing trends in North China Plain,  
171 Sichuan Basin and Yangze River Plain, **but increased mostly in China from 2004 to**  
172 **2012**. A decreasing trend was observed during the year of 2008 and 2009, especially in  
173 Northern China Plain. This may be due to a combination of Chinese economic  
174 downturn and emission reduction during the Olympic games (Lin and McElroy, 2011)  
175 (Wang et al., 2010). **Anyway, as an important aerosol precursor, NO<sub>2</sub> showed the**  
176 **most increasing trend in China**, consistent with the trend of increased aerosol  
177 concentration **by modeling result (Xing et al., 2015)**. Figure S3 shows the annual trends  
178 of aerosol inorganic fraction in PM<sub>2.5</sub> mass concentration from 1998-2012 with GEOS-  
179 Chem model **combined with satellite** results in China. The results indicate that North  
180 China Plain area suffered the most from heavily pollution, consistent with our surface  
181 observations as well as earlier work (Xin et al., 2015). Aerosol concentrations have  
182 increased considerably from 1980 to 2010. The modeling combined with satellite results by  
183 **Boys et al. (2014)** show that concurrently the fraction of inorganic fraction has increased more  
184 rapidly. **Consequently, the water uptake of the aerosol have increased leading to reduced**  
185 **visibility as we suggested, which is consistent with ground-based observations (Yang et al.,**  
186 **2011).**



### 187 3.3 Validation of increased inorganic aerosol components with elevated air 188 pollution level with in-situ measurement

189 To validate our hypothesis that the increased inorganic components contribute to  
190 visibility degradation, we used four months of aerosol chemical composition and  
191 visibility data from urban Beijing from November of 2010 to February of 2011. As  
192 shown in Figure 5, we divided the visibility values into four bins, which corresponds to  
193 clean time to heavy pollution time and to conditions in between. The inorganic aerosol  
194 precursors of SO<sub>2</sub> and NO<sub>2</sub> nearly doubled as the visibility decreased from more than  
195 10 km (clean time) to less than 2 km (heavily polluted time). At the same time, the mass  
196 concentration of nitrate, sulfate and ammonium components increased to 13.5 μg m<sup>-3</sup>,  
197 15.5 μg m<sup>-3</sup> and 10.6 μg m<sup>-3</sup>, respectively. Meanwhile, the mass fraction of these  
198 inorganics increased from 11.3% to 17.3%, from 13.0% to 19.9% and from 9.6% to  
199 13.6%, respectively. At the same time, the mass concentration and fraction of organic  
200 components changed from 12.2 μg m<sup>-3</sup> to 33.4 μg m<sup>-3</sup> and 60% to 46%, respectively.

201 We also investigated the relationship between relative humidity (RH) and volume  
202 fractions of ammonium sulfate, ammonium nitrate and organic aerosols as shown in Figure 6.  
203 The results indicated that ammonium nitrate increased most significantly in elevated RH. On  
204 the contrary, ammonium sulfate, as another inorganic compound, showed only a moderate  
205 positive correlation with RH and a decrease in the volume fraction was observed in RH values  
206 larger than 75%. This might be associated with liquid phase oxidation of SO<sub>2</sub> under high RH  
207 condition, to sulfate aerosol. Increasing RH may provide more atmospheric oxidants and  
208 reaction media for the aqueous-phase oxidation (Zhang et al., 2015). The volume fraction of  
209 organic aerosol showed negative correlation with increasing RH, as presented in Figure 6 (c),  
210 which was maybe due to an faster increasing volume fraction of inorganic aerosol than organic  
211 aerosol.

212 This direct observation shows that the contribution of inorganic components increased  
213 during this campaign. It is plausible that the increased concentration of SO<sub>2</sub> and NO<sub>2</sub>  
214 are highly associated with this giving rise to the long-term trends observed in Figure 2  
215 (Pan et al., 2016; Wang et al., 2014).

#### 216 **4. Conclusion and implication for atmospheric air pollution control**

217 Atmospheric pollution and associated haze events has a dramatic effect on climate  
218 change, human health and visibility degradation (Ding et al., 2013; Petäjä et al., 2016;  
219 Wang et al., 2015; Zhang et al., 2015). Here, longterm visibility measurements  
220 combined with satellite data sets, in-situ measurements and model results revealed that  
221 increased fractions of inorganic aerosol components in the particle matter are crucial in  
222 contributing to more haze events. In this way, aerosol hygroscopic growth has occurred  
223 in lower relative humidity conditions than before due to more ammonium nitrate  
224 aerosol, and the light scattering ability of atmospheric aerosol enhanced as shown in  
225 Figure 7. Another mechanism is that high concentration of NO<sub>x</sub> can promote the  
226 conversion of SO<sub>2</sub> to form sulfate aerosol via aqueous phase oxidation during intensive  
227 pollution periods (He et al., 2014; Wang et al., 2016). Considering the vast energy  
228 consumption in the future decades and the sources of inorganic components in  
229 atmospheric aerosol, we demonstrate that the reduction nitrate, sulfate, ammonium  
230 and their precursors maybe more critical in China.

231

#### 232 Acknowledgements

233 We acknowledge Dr B. Boys and Professor R. Martin of Dalhousie University for  
234 providing GEOS-Chem model results in China. We thank NOAA and SCIAMACHY

235 team for providing high quality data. This work was supported by the Ministry of Science and  
236 Technology of China (No: 2017YFC0210000), the National Research Program for key issues in  
237 air pollution control (DQGG0101) and Academy of Finland via Center of Excellence in  
238 Atmospheric Sciences and the National Natural Science Foundation of China (41605119).

239

#### 240 **Competing financial interests**

241 The authors declare no competing financial interests.

#### 242 **Author contributions**

243 Y.H.W had the original idea. L.L.W and C.S.G provided and processed satellite and  
244 visibility data. Y.S.W provided measurements of aerosol chemical composition  
245 data. Y.H.W, Y.S.W, L.L.W, T.P and M.K interpreted the data and write the paper.

246 All the authors commented on the paper.

#### 247 **References**

248 Boys, B.L. et al. Fifteen-Year Global Time Series of Satellite-Derived Fine Particulate  
249 Matter. *Environmental Science & Technology*, 48(19): 11109-11118, 2014.

250 DeCarlo, P.F. et al. Field-Deployable, High-Resolution, Time-of-Flight Aerosol Mass  
251 Spectrometer. *Analytical Chemistry*, 78(24): 8281-8289, 2006.

252 Ding, A.J. et al.. Intense atmospheric pollution modifies weather: a case of mixed biomass  
253 burning with fossil fuel combustion pollution in eastern China. *Atmos. Chem. Phys.*,  
254 13(20): 10545-10554, 2013.

255 Fu, G.Q., Xu, W.Y., Yang, R.F., Li, J.B. and Zhao, C.S. The distribution and trends of fog  
256 and haze in the North China Plain over the past 30 years. *Atmos. Chem. Phys.*,  
257 14(21): 11949-11958, 2014.

258 Guo, S. et al. Elucidating severe urban haze formation in China. Proceedings of the National  
259 Academy of Sciences of the United States of America, 111(49): 17373-8, 2014.

260 Hao, J., He, K., Duan, L., Li, J. and Wang, L. Air pollution and its control in China. Frontiers  
261 of Environmental Science & Engineering in China, 1(2): 129-142, 2007

262 He, H. et al. Mineral dust and NO<sub>x</sub> promote the conversion of SO<sub>2</sub> to sulfate in heavy  
263 pollution days. Sci Rep, 4: 4172, 2014.

264 Huang, R.J. et al. High secondary aerosol contribution to particulate pollution during haze  
265 events in China. Nature, 514(7521): 218-22, 2014.

266 Jimenez, J.L. et al. Evolution of Organic Aerosols in the Atmosphere. Science, 326(5959):  
267 1525-1529, 2009.

268 Kulmala, M.. Build a global Earth observatory. Nature, 553, 2018.

269 Kulmala, M.. China's choking cocktail. Nature, 526, 2015.

270 Kulmala M., L.K., Virkkula A., Petäjä T., Paasonen P., Kerminen V.-M., Nie W., Qi X., Shen  
271 Y., Chi X. & Ding A. On the mode-segregated aerosol particle number concentration  
272 load: contributions of primary and secondary particles in Hyytiälä and Nanjing.  
273 Boreal Env. Res, 21: 319–331, 2016.

274 Lelieveld, J., Evans, J.S., Fnais, M., Giannadaki, D. and Pozzer, A. The contribution of  
275 outdoor air pollution sources to premature mortality on a global scale. Nature,  
276 525(7569): 367-71, 2015.

277 Lin, J.T. and McElroy, M.B. Detection from space of a reduction in anthropogenic emissions  
278 of nitrogen oxides during the Chinese economic downturn. Atmos. Chem. Phys.,  
279 11(15): 8171-8188, 2011.

280 Pan, Y. et al. Redefining the importance of nitrate during haze pollution to help optimize an  
281 emission control strategy. Atmospheric Environment, 141: 197-202, 2016.

282 Peng, J. et al. Markedly enhanced absorption and direct radiative forcing of black carbon  
283 under polluted urban environments. Proceedings of the National Academy of  
284 Sciences, 113(16): 4266-4271, 2016.

285 Petäjä, T. et al. Enhanced air pollution via aerosol-boundary layer feedback in China.  
286 Scientific Reports, 6: 18998, 2016.

287 Richter, A., Burrows, J.P., Nusz, H., Granier, C. and Niemeier, U. Increase in tropospheric  
288 nitrogen dioxide over China observed from space. Nature, 437(7055): 129-132, 2005.

289 Swietlicki, E. et al. Hygroscopic properties of submicrometer atmospheric aerosol particles  
290 measured with H-TDMA instruments in various environments—a review. Tellus B:  
291 Chemical and Physical Meteorology, 60(3): 432-469, 2008.

292 van Donkelaar, A. et al. Global estimates of ambient fine particulate matter concentrations  
293 from satellite-based aerosol optical depth: development and application.  
294 Environmental health perspectives, 118(6): 847-855, 2010.

295 Wang, G. et al.. Persistent sulfate formation from London Fog to Chinese haze. Proceedings  
296 of the National Academy of Sciences, 113(48): 13630-13635, 2016.

297 Wang, S. et al. Quantifying the Air Pollutants Emission Reduction during the 2008 Olympic  
298 Games in Beijing. Environmental Science & Technology, 44(7): 2490-2496, 2010.

299 Wang, Y. et al. Mechanism for the formation of the January 2013 heavy haze pollution  
300 episode over central and eastern China. Science China Earth Sciences, 57(1): 14-25,  
301 2014.

302 Wang, Y.H. et al. Aerosol physicochemical properties and implications for visibility during  
303 an intense haze episode during winter in Beijing. Atmos. Chem. Phys., 15(6): 3205-  
304 3215, 2015.

305 Wu, Y. et al. The challenge to NO<sub>x</sub> emission control for heavy-duty diesel vehicles in China.  
306 Atmos. Chem. Phys., 12(19): 9365-9379, 2012.

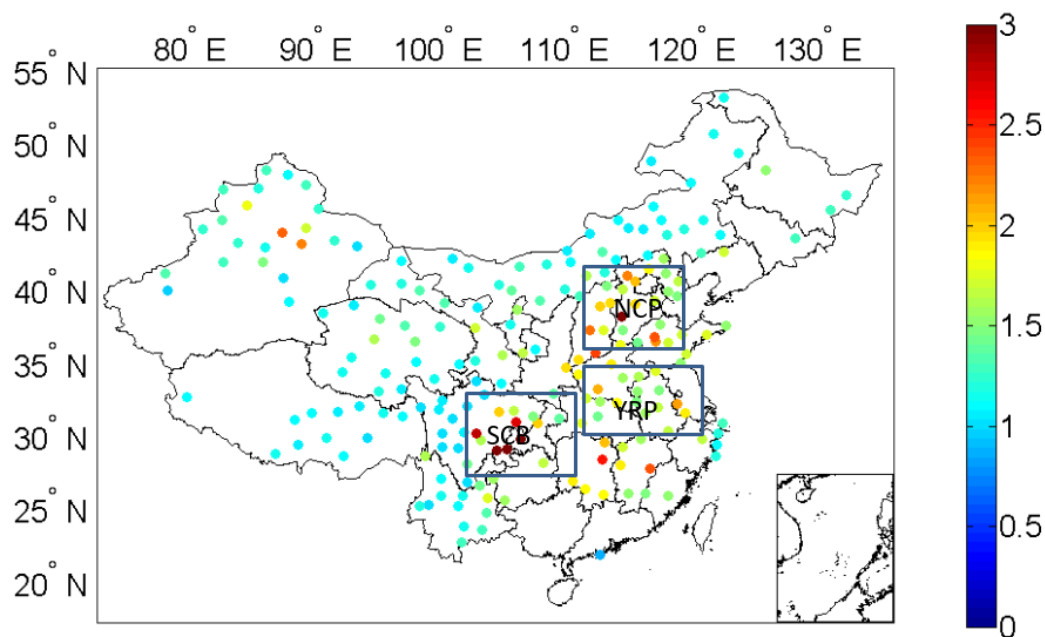
307 Xin, J. et al. The Campaign on Atmospheric Aerosol Research Network of China: CARE-  
308 China. Bulletin of the American Meteorological Society, 96(7): 1137-1155. 2015.

309 Xing, J. et al. Observations and modeling of air quality trends over 1990–2010 across the  
310 Northern Hemisphere: China, the United States and Europe. Atmos. Chem. Phys.,  
311 15(5): 2723-2747, 2015.

312 Yang, F. et al. Characteristics of PM<sub>2.5</sub> speciation in representative megacities and across  
313 China. *Atmos. Chem. Phys.*, 11(11): 5207-5219, 2011.  
314 Zhang, J.K. et al. Characterization of submicron aerosols during a month of serious pollution  
315 in Beijing, 2013. *Atmos. Chem. Phys.*, 14(6): 2887-2903, 2014.  
316 Zhang, R. et al. Formation of urban fine particulate matter. *Chem Rev*, 115(10): 3803-55,  
317 2015  
318 Zhang, X.Y. et al. Atmospheric aerosol compositions in China: spatial/temporal variability,  
319 chemical signature, regional haze distribution and comparisons with global aerosols.  
320 *Atmos. Chem. Phys.*, 12(2): 779-799, 2012.

321

322 **Figure caption**



323

324 **Figure 1.** The distribution of the average surface visibility ratio in dry and wet  
325 conditions based on observations at 262 surface observation sites in China. The  
326 aerosol in the industrialized regions of China in the East are more hygroscopic than  
327 aerosol particles in the west of China.

328

329

330

331

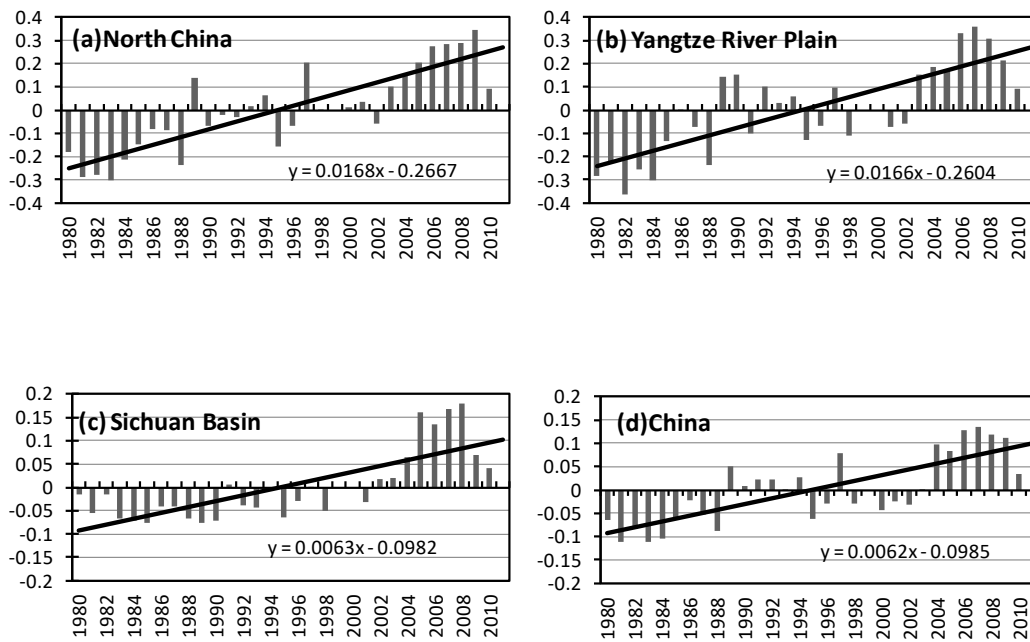
332

333

334

335

336



337

338 **Figure 2.** Anomalies and trends of ratio of visibility in North China Plain, Yangtze  
339 Plain, Sichuan Basin and in China as a whole. The relative contribution of  
340 hygroscopic aerosols to the visibility reduction has increased from 1980 to 2010 in  
341 China.

342

343

344

345

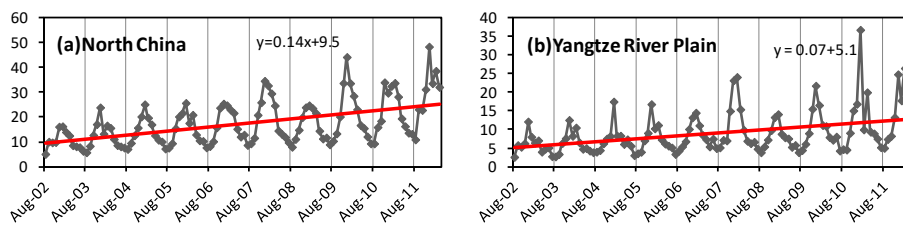
346

347

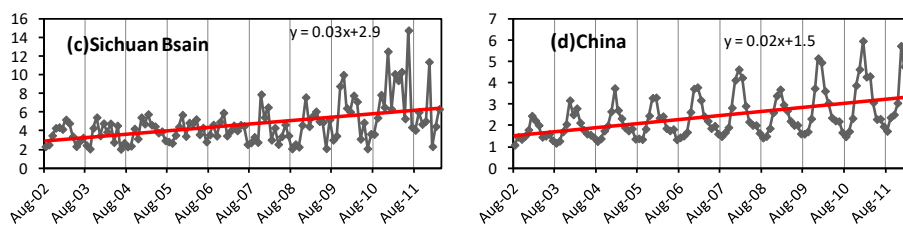
348

349

350



351



352 Figure 3. Trends of NO<sub>2</sub> concentration over china from SCIAMACHY from the year

353 2002 to 2012 ( $10^{15}$  mol/cm<sup>2</sup>)

354

355



356

357

358

359

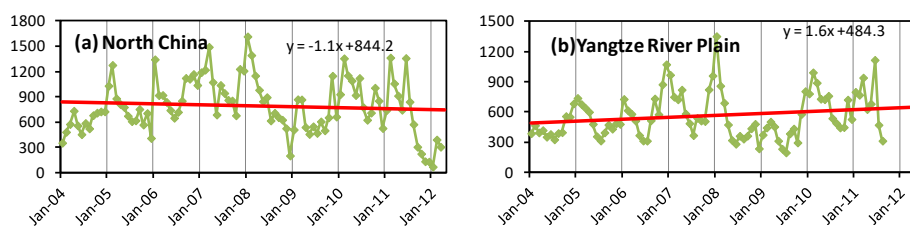
360

361

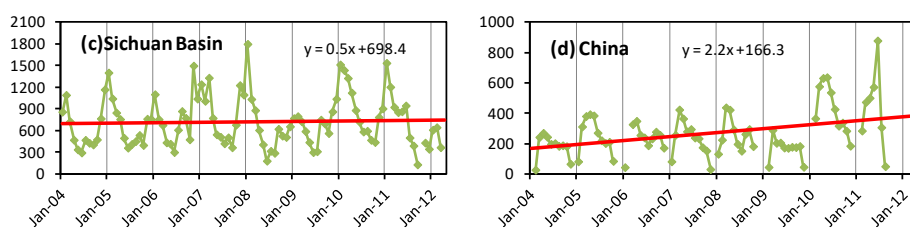
362

363

364



365



366

Figure 4. Trends of SO<sub>2</sub> concentration over china from SCIAMACHY from the year of

367

2004 to 2012 (1000DU)

368

369

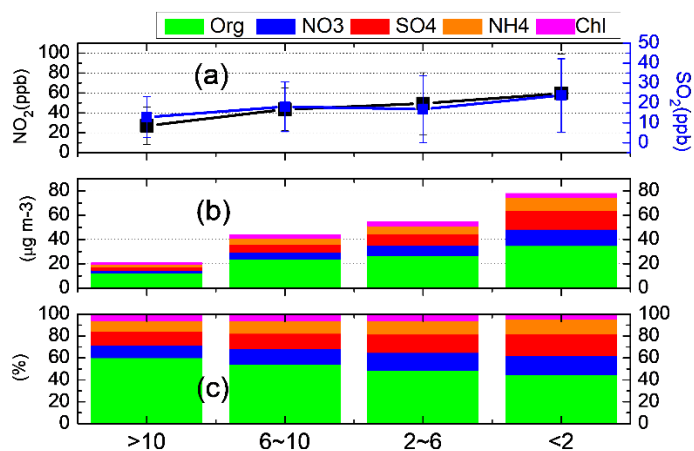
370

371

372

373

374



375

376

377

378

379 **Figure 5:** Variation of (a) NO<sub>2</sub>, SO<sub>2</sub>, (b) chemical composition (c) mass fraction of  
380 organic, nitrate, sulfate, ammonium and chloride with decreased visibility during the  
381 intensive campaign in Beijing.

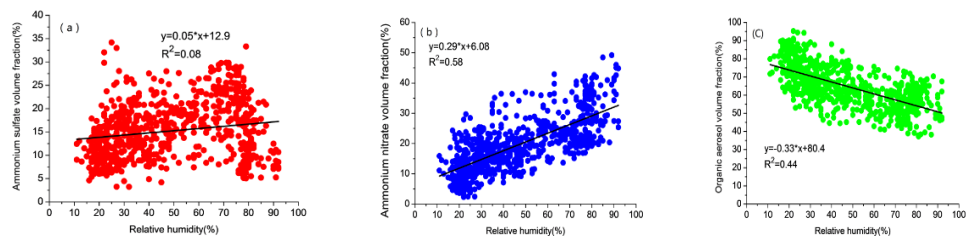
382

383

384

385

386



387

388 Figure 6. Relation between relative humidity (RH) and volume fractions of (a) ammonium

389 sulfate (b) ammonium nitrate (c) organic aerosol.

390

391

392

393

394

395

396

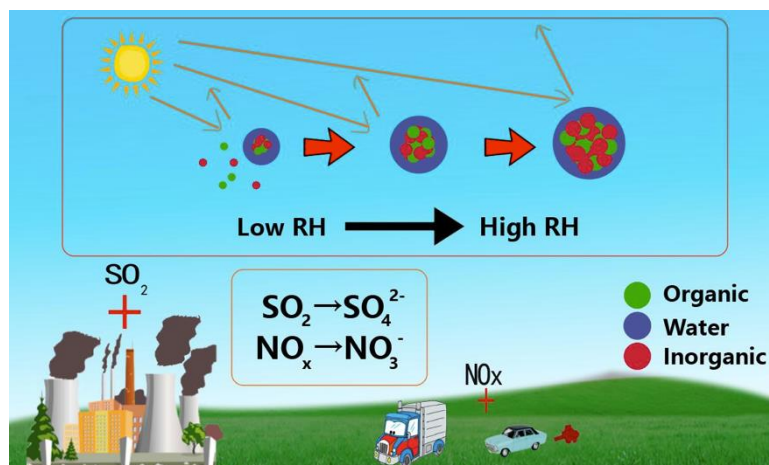
397

398

399

400

401



402

403        Figure 7. A schematic picture illustrating the process of enhanced emission of  
404 aerosol inorganic precursors and formation of aerosol inorganic components leading to  
405 increased hygroscopicity and aerosol water uptake ability leading to considerable  
406 visibility degradation in China. The plus symbols represents the strengthening of a  
407 specific process.

408

409